Minocycline Promotes Functional Recovery in Ischemic Stroke by Modulating Microglia Polarization Through STAT1/STAT6 Pathways

Yunnan Lu
Xishan People's Hospital of Wuxi City
Mingming Zhou
Taihu University of Wuxi
Yun Li
Nanjing Medical University
Yan Li
Nanjing Medical University
Ye Hua
Affiliated Wuxi Clinical College of Nantong University
Yi Fan (Yfan@njmu.edu.cn)
Nanjing Medical University https://orcid.org/0000-0003-1783-3220

Research

Keywords: Minocycline, ischemic stroke, microglia, neuroinflammation, STAT1, STAT6

Posted Date: January 5th, 2021

DOI: https://doi.org/10.21203/rs.3.rs-138254/v1

Abstract

Background

Increasing evidence suggests that microglia experience two distinct phenotypes after acute ischemic stroke (AIS): a deleterious M1 phenotype and a neuroprotective M2 phenotype. Promoting the phenotype shift of M1 microglia to M2 microglia is thought to improve functional recovery after AIS. Minocycline, a tetracycline antibiotic, can improve functional recovery after cerebral ischemia in pre-clinical and clinical research. However, the role and mechanisms of minocycline in microglia polarization is unclear.

Methods

Using the transient middle cerebral artery occlusion - reperfusion (MCAO/R) model, we treated mice with saline or different minocycline concentration (10, 25, or 50 mg/kg, i.p., daily for 2 wk) at 24 h after reperfusion. Neurobehavioral evaluation, rotarod test, and corner turning test were carried out on day 14 after reperfusion. Then, neuronal injury, reactive gliosis, and microglia polarization were performed on day 7 following MCAO/R. Finally, we treated primary microglial cultures with LPS (Lipopolysaccharide; 100 ng/mL) plus IFN-γ (20 ng/mL) 24 h to induce M1 phenotype and observed the effects of minocycline on the M1/M2-related mRNAs and the STAT1/STAT6 pathway.

Results

We found that a 14-day treatment with minocycline increased the survival rate and promoted functional outcomes evaluated with neurobehavioral evaluation, rotarod test, and corner turning test. Meanwhile, minocycline reduced the brain infarct volume, alleviated neuronal injury, and suppressed reactive gliosis on day 7 following MCAO/R. Moreover, we observed an additive effect of minocycline on microglia polarization to the M1 and M2 phenotypes *in vivo* and *in vitro*. In the primary microglia, we further found that minocycline prevented neurons from OGD/R-induced cell death in neuron-microglia co-cultures via regulating M1/M2 microglia polarization through the STAT1/STAT6 pathway.

Conclusion

Minocycline promoted microglial M2 polarization and inhibited M1 polarization, leading to neuronal survival and neurological functional recovery. The findings deepen our understanding of the mechanisms underlying minocycline-mediated neuroprotection in AIS.

Background

Acute ischemic stroke (AIS), a leading cause of death and disability worldwide, accounts for approximately 85% of total stroke [1]. Intravenous thrombolysis with recombinant tissue-type plasminogen activator (IV-tPA) remains the only approved thrombolytic medication for treating AIS [2]. At present, endovascular treatment, particularly intra-arterial thrombolysis and thrombectomy, is a possible treatment option for AIS patients when initial IV-tPA fails [3]. However, some clinical trials found that

endovascular therapy can not improve disability-free survival after AIS compared with IV-tPA, indicating that infarcted tissue is technically successful recanalization but no longer salvageable [4, 5]. Thus, medicines for effective stroke recovery are likely to remain an essential part of stroke care in the future.

Post-stroke inflammation plays an essential role in the survival and regeneration of nerve cells after AIS [6, 7]. The lack of oxygen and energy during AIS leads to rapidly damaging nervous tissue and activates the innate immune system to support healing, including clearing the dead tissue. Brain-resident microglia and infiltrating peripheral leukocytes migrate to the infarct area and stimulate the production and secretion of pro-inflammatory cytokines. These immune cells contribute to the clearance of cellular debris and dead cells from the injured brain through phagocytosis. However, they also destroy salvageable tissue, which is only damaged by the lack of oxygen and energy not yet dead. Thus, post-stroke inflammation is both detrimental and beneficial at different stages [8]. The proper function of these immune cells is fundamental to post-stroke recovery.

Microglia mediates the inflammatory cascades as the first defensive line and modulates brain repair after stroke [8, 9]. Increasing evidence suggests microglia could experience two distinct phenotypes after activation: a "classical" deleterious M1 phenotype stimulated by lipopolysaccharide (LPS) and interferon-γ (IFN-γ) and an "alternative" neuroprotective M2 phenotype stimulated by interleukin-4 (IL-4) [10]. After AIS, M1 microglia promotes inflammation and aggravates brain damage by releasing pro-inflammatory mediators at the injury site where the repair process of M2 microglia is depressed. Thus, promoting the phenotype shift of M1 to M2 has become an adjunct therapy in recovery after stroke [11, 12].

Minocycline, an anti-infective agent of the tetracycline family, was known for its anti-inflammatory effects in neurological disorders [13-15], including AIS [16]. We previously found that minocycline could prevent microglia activation and inhibit the NLRP3 inflammasome up to 72 h after the transient middle cerebral artery occlusion - reperfusion (MCAO/R) [17]. Since it is reported that minocycline can improve functional recovery after cerebral ischemia [18, 19], we have a hypothesis that minocycline may shift microglia from M1 to M2 phenotype in recovery after induction of MCAO/R.

Materials And Methods

Animals and treatment

Male C57BL/6 mice (aged 10–12 weeks, weighing 23–25 g) were purchased from the Animal Core Facility of Nanjing Medical University. All mice were housed in five per cage groups in a standardized light-dark cycle at 22 °C and given free access to food and water. All experimental procedures were approved by the Institutional Animal Care and Use Committee of Nanjing Medical University. All procedures were designed to minimize suffering and reduce the number of animals used.

MCAO/R model

MCAO/R mice were established as previously described [17]. For the transient model, reperfusion was produced by withdrawal of the 6-0 nylon filament (Doccol Corp., Readlands, CA, USA) 60 min after the occlusion. In the sham group, arteries were visualized but not ligated. After the surgery, body temperature was controlled with a heating pad and kept at 37 ° C until mice wholly recovered from anesthesia. The mice were then returned to their home cages.

Grouping and treatment

After 24 h of reperfusion, the model mice were subjected to neurological function evaluation based on the neurological severity scores (NSS) system. Mice with NSS scores of 4 to 10 were randomly divided into 4 groups and received intraperitoneal injections with saline, minocycline 10 mg/kg, 20 mg/kg, or 50 mg/kg. They were then sacrificed on days 3, 7, or 14 after reperfusion according to different experimental purposes. Minocycline (Sigma-Aldrich, St. Louis, MO, USA) was freshly diluted to the concentrations needed with saline.

Neurobehavioral function evaluation

Using the revised NSS system [20], the neurobehavioral evaluation of mice was examined by two trained observers who were blinded to the drug treatment group. According to the NSS presented in Table 1, mice's neurological status was examined on day 1 and day 14 following MCAO/R (Fig. 1a). The 1-day assessment was used to verify the ischemic state of MCAO/R groups. The 14-day assessment was used to evaluate motor and behavioral impairments in recovery after induction of MCAO/R.

Rotarod test

We carried out the rotarod test to calculate mice's motor ability as previously described [21]. All mice were acclimatized to the rotarod by undergoing a 3-day training program before MCAO/R surgery experiments. Only mice that can remain on the rotarod for 180 s were used for the experiments. On day 14 following MCAO/R, mice performed three trials on the rotarod, with an interval of 5 min. The mean of the three trials was used to show the functional recovery of mice.

Corner turning test

The corner test was performed as previously described [22]. Briefly, a mouse was left in the test device consisting of two vertical boards at a 30° angle. When the mouse entered the corner, the direction in which it contacted the board with the vibrissae was recorded. The non-ischemic mouse turned left or right with equal frequency, but the mouse suffered from MCAO/R preferentially turned toward the impaired (right side in our experiment). The number of turns in each direction was summed from 10 trials. The following formula was used to calculate right-biased turning percentage: right-biased turning percentage = right-biased turning / total turning × 100%.

TTC assay

As previously described [21], the cerebral infarct volume of nine mice in each group was measured with 1% TTC (dissolved in saline) on day 7 following MCAO/R. The infarcted regions were acquired by a digital camera and quantified using ImageJ software (NIH, Bethesda, MD, USA). The following formula was used to calculate infarct percentage: Infarct percentage = infarct volume/volume of the contralateral hemisphere × 100%.

Immunohistochemistry and cell counting

On day 3 or day 7 following MCAO/R, six mice were anesthetized with pentobarbital sodium (80 mg/kg) and then perfused with saline and 4% paraformaldehyde as previously described [21]. Their brains were fixed overnight in 4% paraformaldehyde at 4 °C, followed by dehydration in 30% w/v sucrose at 4 °C. The frozen coronal sections of 30 μm were cut with a vibrating microtome (Leica CM1950, Nussloch, Germany).

For immunohistochemistry, the sections were incubated with primary antibody against NeuN (1:1000, #MAB377; Millipore, Billerica, MA, USA), GFAP (1:1000, #ab53554; Cambridge, MA, USA), and Iba-1 (1:500, #019-19741; Wako, Osaka, Japan) at 4 °C overnight. After incubated with corresponding secondary antibodies for one hour at room temperature, the sections were incubated with 3,3'-diaminobenzidine (DAB) staining (Beyotime, Shanghai, China). The total numbers of $NeuN^+$, $GFAP^+$, and $Iba\text{-}1^+$ cells were estimated with an optical dissector (Stereo Investigator, MicroBright Field. Inc., Williston, VT, USA) as described previously [23].

For immunofluorescence, the sections were incubated with primary antibody against Iba-1, CD16/32 (1:50, #553142BD; Biosciences Pharmingen, San Jose, CA, USA), and CD206 (1:50, #AF2535; R&D Systems, Minneapolis, MN, USA). After incubation with corresponding Alexa Fluor secondary antibodies, the sections were mounted with ProLong Gold antifade reagent (#P36930, Life Technologies, Carlsbad, CA, USA). Quantitative assessment of co-localization between Iba-1 and CD16/32 or CD206 was performed by calculating the positive cells in every 6th section containing ten preassigned fields in the penumbra using a fluorescence microscope (AX10, Carl Zeiss, Thornwood, NY, USA).

Quantitative real-time polymerase chain reaction

Quantitative real-time polymerase chain reaction (qRT-PCR) was performed as previously described [24]. Briefly, total RNA from penumbral tissue or culture cells was purified using the Trizol extraction method. Real-time qPCR of cDNA was carried out using SYBR Green detection on the ABI 9600 (Applied Biosystems, Foster City, CA, USA). The qRT-PCR primers for IL-1β (#MQP092978), IL-6 (#MQP088375), iNOS (#MQP088374), TNF-α (#MQP096302), Arg1 (#MQP026580), IL-10 (#MQP092952), TGF-β (#MQP088616), Ym1 (#MQP091480), and GAPDH (#MQP027158) were purchased from GeneCopoeia, Inc. (Rockville, MD, USA).

Enzyme-linked immunosorbent assay

The protein levels of IL-1β (#CSB-E08054m, Cusabio Biotech Co., Wuhan, Hubei, China), TNF-α (#CSB-E04741m, Cusabio Biotech Co., Wuhan, Hubei, China), IL-10 (#CSB-E04594m, Cusabio Biotech Co., Wuhan, Hubei, China), and TGF-β (#CSB-E04726m, Cusabio Biotech Co., Wuhan, Hubei, China) from tissues or culture cells were quantitated by a specific enzyme-linked immunosorbent assay (ELISA) kit following the manufacturer's instructions.

Cell culture and treatment

Primary microglia from cerebral cortex of newborn mice were cultured and isolated as previously described [25]. At days in vitro (DIV) 10, microglia cells were seeded on 6-well plates and incubated with 100 ng/mL LPS (Sigma-Aldrich, St. Louis, MO, USA) plus 20 ng/mL IFN-γ (PeproTech, Suzhou, China) followed by 50 μM minocycline or saline for 24 h.

Western blot analysis

The cells were lysed in lysis buffer (50 mM Tris-HCl, 150 mM NaCl, 1% Nonidet P-40, 1 % sodium orthovanadate, 5 mM EDTA, pH 7.4,) containing protease inhibitors and phosphatase inhibitors (Roche Applied Science, Indianapolis, IN, USA). The proteins were separated by 10% SDS-PAGE and transferred to PVDF membranes with the electrophoretic transfer system (Bio-Rad Laboratories, Hercules, CA, USA). Nonspecific blots were blocked with 5 % skimmed milk in Tris-buffered saline with 0.1 % Tween 20 (TBST) for 1 h. The membranes were then incubated with the following primary antibodies: iNOS (1:100, #ab178945; Abcam Inc., Cambridge, UK), p-P65 (1:1000, #3033; Cell Signaling Technology Inc., Danvers, MA, USA), P65 (1:2000, #8242; Cell Signaling Technology Inc., Danvers, MA, USA), p-STAT1 (1:1000, #7649; Cell Signaling Technology Inc., Danvers, MA, USA), STAT1 (1:2000, #14995; Cell Signaling Technology Inc., Danvers, MA, USA), Arg1 (1:1000, #ab124917; Abcam Inc., Cambridge, UK), p-STAT6 (1:2000, #9364; Cell Signaling Technology Inc., Danvers, MA, USA), STAT6 (1:2000, #5397; Cell Signaling Technology Inc., Danvers, MA, USA), or β-actin (1:10000, #YFMA0052; Yifeixue Biotech, Nanjing, China) overnight at 4°C. The membranes were washed and incubated with corresponding secondary antibodies for 1 h at room temperature. Finally, the membrane was observed and analyzed with Tanon 5200 (Tanon Science and Technology Co. Ltd, Shanghai, China).

Neuron-microglia co-culture

Primary microglia and cortical neurons were co-cultured in a two-layer system (Transwell, Corning, Corning, NY, USA). Briefly, microglia on Transwell inserts were treated with 100 ng/mL LPS plus 20 ng/mL IFN-γ followed by 50 μM minocycline or saline for 24 h. Then, the medium was removed and washed with fresh medium three times. Primary cortical neurons were cultured and subjected to oxygen-glucose deprivation/reperfusion (OGD/R) for 1 h, as previously described [24]. When the medium was replaced with a normal medium, the microglia inserts were added on top of neuronal cultures to generate a neuron-microglia co-cultures. After 24 h of co-culture, neuronal cell death and survival were measured by thiazolyl blue tetrazolium bromide (MTT; Sigma-Aldrich, St. Louis, MO, USA) assay and lactate

dehydrogenase (LDH) assays (Nanjing Jiancheng Bioengineering Institute, Nanjing, China) according to the manufacturer's protocol.

Statistical analysis

All data were expressed as mean ± S.E.M. Statistical analysis was performed using GraphPad Prism software (San Diego, CA, USA). A log-rank test was used to compare the survival rate of the MCAO/R model. A non-parametric Kruskal-Wallis H-test was used to compare the NSS scores of the MCAO/R model. Other parametric data were analyzed via one-way analysis of variance (ANOVA) followed by Tukey's test or a two-sample *t*-test. $P < 0.05$ was considered statistically significant.

Results

Minocycline enhanced functional recovery after MCAO/R model

To confirm the effects of minocycline on functional recovery following AIS, we treated mice subjected to MCAO/R with saline or different minocycline concentration (10, 25, or 50 mg/kg, *i.p.*, daily for 2 wk) at 24 h after reperfusion (Fig. 1a). No mice died during the surgery. During the first 1 wk after reperfusion, 18 mice in MCAO/R group, 11 mice in MCAO/R + 10 mg/kg minocycline group, 8 mice in MCAO/R + 20 mg/kg minocycline group, and 3 mice in MCAO/R + 50 mg/kg minocycline group died. Since mice that survived did not die during the time window of 14 days, the survival rate was 45.5%, 56.0%, 68.0%, and 88.0%, respectively (Fig. 1b). The survival rate was significantly different among groups ($P = 0.0019$), and between MCAO/R group and MCAO/R + 50 mg/kg minocycline group ($P = 0.0016$).

To evaluate the initial neurological deficit after MCAO/R and monitor neurobehavior on day14 after minocycline treatment, we rated each mouse's performance suffered from MCAO/R according to NSS scores. The mice suffered from MCAO/R showed high neurological deficit scores at d 1 after reperfusion (Fig. 1c, open column). There was no difference among the four groups ($P = 0.9716$). At day 14 after minocycline treatment, three MCAO/R + minocycline groups demonstrated less neurological impairment compared to MCAO/R + saline group, and the mice treated with 25 mg/kg ($P = 0.0001$) and 50 mg/kg ($P < 0.0001$) minocycline showed a significant difference (Fig. 1c). Consistent with the NSS scores, the mice in MCAO/R + minocycline groups showed increased latency time in the rotarod test (Fig. 1d). The latency time was significantly different among groups ($F(4, 77) = 42.83$, $P < 0.0001$), between MCAO/R + saline group and MCAO/R + 25 mg/kg minocycline group ($P = 0.0003$), and between MCAO/R + saline group and MCAO/R + 50 mg/kg minocycline group ($P < 0.0001$). Meanwhile, the mice in MCAO/R + minocycline groups also showed reduced right-biased turning in corner turning test (Fig. 1e). The percentage of right-biased turning was significantly different among groups ($F(4, 77) = 41.41$, $P < 0.0001$), between MCAO/R + saline group and MCAO/R + 25 mg/kg minocycline group ($P < 0.0001$), and between MCAO/R + saline group and MCAO/R + 50 mg/kg minocycline group ($P < 0.0001$). These results indicate that minocycline improves functional motor recovery at d 14 following MCAO/R.

Minocycline alleviated neuronal injury on day 7 following MCAO/R

Since mice did die during the time window of the first 7 days, we chose day 7 after reperfusion to observe the effects of minocycline on neuronal injury after MCAO/R (Fig. 2a).

The infarct size of four MCAO/R groups was first measured by TTC staining (Fig. 2b). The infarct sizes was significantly different among groups (F (3, 32) = 4.388, P = 0.0107) and between MCAO/R + saline group and MCAO/R + 50 mg/kg minocycline group (P = 0.0085). Minocycline reduces the brain infarct volume on day 7 following MCAO/R.

To further evaluate the neuroprotective role of minocycline in post-stroke rehabilitation, we analyzed neuronal cell death in the cortex (Fig. 2c) and striatum (Fig. 2d) using immunohistochemistry against NeuN. The numbers of $NeuN^+$ cells in the cortex of mice suffered from MCAO/R decreased to 35.2% (41697 ± 3105 *vs.* 118505 ± 10977, P < 0.0001) in the ipsilateral and 75.4% (86967 ± 7068 vs. 115341 ± 12289, P = 0.2332) in the contralateral compared to that in sham mice. The numbers of $NeuN^+$ cells in the 50 mg/kg minocycline treatment group significantly increased by 226.1% (94280 ± 9261, P = 0.0015) in the ipsilateral cortex. Consistent with the cortex, the numbers of $NeuN^+$ cells in the striatum of mice suffered MCAO/R decreased to 26.7% (34990 ± 2258 *vs.* 131080 ± 13406, P = 0.0001) in the ipsilateral striatum and 71.2% (91182 ± 7780 vs. 128120 ± 8722, P = 0.0228) in the contralateral striatum. The numbers of $NeuN^+$ cells in the 50 mg/kg minocycline treatment group significantly increased by 330.0% (115370 ± 15792, P = 0.0007) in the ipsilateral striatum and by 143.2% (130550 ± 9493, P = 0.0154) in the contralateral striatum. These results indicate that minocycline promotes neuronal survival on day 7 following MCAO/R.

Minocycline reduced reactive gliosis on day 7 following MCAO/R

To evaluate the impact of reactive gliosis on neuronal loss in MCAO/R, we analyzed the density of activated astrocytes ($GFAP^+$ cells) and reactive microglia ($Iba\text{-}1^+$ cells). The density of $GFAP^+$ cells of mice suffered from MCAO/R was significantly increased by 244.0% (15226 ± 1320 *vs.* 6239 ± 419, P < 0.0001) in the ipsilesional cortex and by 380.0% (13671 ± 1387 *vs.* 3599 ± 391, P < 0.0001) in the ipsilesional striatum (Fig. 3a). A 7-day course of minocycline significantly reduced the density of $GFAP^+$ cells by 49.2% (7492 ± 611, P < 0.0001) in the ipsilesional cortex and by 29.1% (3979 ± 478, P < 0.0001) in the ipsilesional striatum. Additionally, resting microglia was defined by the characteristic ramified shape, while activated microglia/macrophages showed amoeboid morphology (Fig. 3b). The density of $Iba\text{-}1^+$ cells of mice suffered from MCAO/R was significantly increased by 472.3% (12252 ± 823 *vs.* 2594 ± 265, P < 0.0001) in the ipsilesional cortex and by 759.2% (18229 ± 942 *vs.* 2401 ± 113, P < 0.0001) in the ipsilesional striatum. A 7-day course of minocycline significantly reduced the density of $GFAP^+$ cells by 51.7% (6339 ± 287, P < 0.0001) in the ipsilesional cortex and by 44.2% (8049 ± 319, P < 0.0001) in the ipsilesional striatum. These results suggest that minocycline suppresses reactive gliosis on day 7 following MCAO/R.

Minocycline promoted M2 macrophage/microglia polarization on day 7 following MCAO/R

Due to an M2 to M1 shift in microglia/macrophage phenotype at days 2-7 following ischemia, we further chose day 3 and day 7 after reperfusion to observe the effects of minocycline on microglial polarization dynamics after MCAO/R (Fig. 4a). As previously reported [26], the Iba-1$^+$ microglia/macrophage was recruited to the penumbra on day 3 and then moved to the ischemia core once necrotic debris was phagocytosed on day 7 (Fig. 4b). Consistent with infarct sizes, the MCAO/R mice treated with minocycline displayed the reduction of ischemia core area surrounded by Iba-1$^+$ cells on day 3 and filled by amoeboid-like microglia on day 7. Furthermore, both CD16/32 (Fig. 4c) and CD206 (Fig. 4d) were detected in the penumbra and the ischemia core on day 7 after MCAO/R, indicated an M1/M2 polarization microglia/macrophages in the ipsilateral hemisphere of MCAO/R mice. We found that the percentage of CD16/32$^+$ cells (71.3% ± 3.28%) to the Iba-1$^+$ cells in the penumbral was much larger than the percentage of CD206$^+$ cells (21.2% ± 3.07%) on day 7 after MCAO/R (Fig. 4e). Minocycline treatment significantly reduced the percentage of CD16/32$^+$ cells by 44.6% (31.8% ± 2.26%, $P < 0.001$) and increased the percentage of CD206$^+$ cells by 269.2% (56.8% ± 3.40%, $P < 0.001$).

Furthermore, we performed qRT-PCR and ELISA experiments to detect the expression and production of pro-inflammatory cytokines in the MCAO/R model. The expressions of M1-related mRNAs, including IL-1β ($P = 0.0200$), IL-6 ($P = 0.0005$), iNOS ($P = 0.0015$), and TNF-α ($P = 0.0007$), from the ipsilateral hemisphere of MCAO/R mice were significantly increased compared to the sham group (Fig. 4f). Meanwhile, the levels of M2-related mRNAs, including Arg1 ($P = 0.0031$), IL-10 ($P = 0.0001$), TGF-β ($P = 0.0011$), and Ym1 ($P = 0.0004$), were also significantly enhanced by MCAO/R stimulation (Fig. 4g). The 7-day treatment with minocycline significantly suppressed the mRNA levels of IL-1β ($P = 0.0259$), IL-6 ($P = 0.0445$), iNOS ($P = 0.0090$), and TNF-α ($P = 0.0035$) while promoting the increase of Arg1 ($P = 0.0265$), IL-10 ($P = 0.0386$), TGF-β ($P = 0.0015$), and Ym1 ($P = 0.0008$). Consistent with these gene expressions, MCAO/R injury induced the production of IL-1β ($P < 0.0001$), TNF-α ($P < 0.0001$), IL-10 ($P = 0.0009$), and TGF-β ($P = 0.0020$) (Fig. 4h). Minocycline significantly inhibited the production of M1 cytokines IL-1β ($P = 0.0253$) and TNF-α ($P < 0.0001$) while increasing the production of M2 cytokines IL-10 ($P < 0.0001$) and TGF-β ($P < 0.0001$). These results indicate that minocycline promote M2 polarization of microglia/macrophage polarization to protect against ischemic stroke.

Minocycline facilitated microglia M2 polarization stimulated *in vitro*

Since cerebral ischemia mainly activated and polarized into the M1 phenotype of microglia [26], we treated primary microglial cultures with LPS (100 ng/mL) plus IFN-γ (20 ng/mL) 24 h to induce M1 phenotype. LPS plus IFN-γ treatment increased the expression of pro-inflammatory cytokines IL-1β ($P < 0.0001$), IL-6 ($P < 0.0001$), iNOS ($P < 0.0001$), and TNF-α ($P < 0.0001$) (Fig. 5a) and the productions of IL-1β ($P < 0.0001$) and TNF-α ($P < 0.0001$) (Fig. 5b), indicating microglia to the M1 phenotype. We also found that LPS plus IFN-γ treatment decreased the expression of M2-related mRNA Arg1 ($P = 0.0004$) in primary microglia. Minocycline not only significantly suppressed the expression of IL-1β ($P < 0.0001$), IL-6 ($P < 0.0001$), iNOS ($P < 0.0001$), and TNF-α ($P < 0.0001$) (Fig. 5a) and reduced the production of IL-1β ($P < 0.0001$) and TNF-a ($P < 0.0001$) (Fig. 5b), but also expectedly induced higher mRNA expression of Arg1 (P

< 0.0001), IL-10 (P < 0.0001), TGF-β (P < 0.0001), and Ym1 (P < 0.0001) (Fig. 5c) and secreted higher M2-related cytokines IL-10 (P < 0.0001) and TGF-β (P < 0.0001) (Fig. 5d). Thus, these data *in vitro* demonstrate that minocycline prevente LPS/IFN-γ-activated M1 microglial and facilitates microglial polarization to the M2 phenotype.

Minocycline regulated microglia M1/M2 polarization via the STAT1/STAT6 signaling pathway

In M1/M2 microglia polarization, the STAT1/STAT6 pathway is one of the major signaling pathways and regulates the transcription of M1 or M2 genes following recognition of IFN-γ [27]. To understand the underlying mechanism of the M2 phenotype switch after minocycline treatment, we then observed the effects of minocycline on the STAT1/STAT6 pathway. Microglia were isolated and treated with LPS plus IFN-γ for activating the STAT1 pathway, which is necessary for M1 polarization. Western blot analysis was performed to detect the protein level of iNOS, p-P65, P65, p-STAT1, and STAT1 (Fig. 6a). LPS plus IFN-γ treatment robustly increased the expression of iNOS (P < 0.0001; Fig. 6b) and the phosphorylation of P65 (P < 0.0001; Fig. 6c) and STAT1 (P < 0.0001; Fig. 6d). Quantification analysis showed that minocycline significantly reduced the intensities of iNOS (P < 0.0001; Fig. 6b), p-P65 (P < 0.0001; Fig. 6c), and p-STAT1 (P < 0.0001; Fig. 6d) stimulated by LPS plus IFN-γ. We then detected the protein level of Arg1 and the phosphorylation of STAT6, which is necessary for M2 polarization (Fig. 6a). Quantification analysis showed that minocycline treatment increased Arg1 levels (P < 0.0001; Fig. 6e) and activated the phosphorylation of STAT6 (P < 0.0001; Fig. 6f). The results indicate that minocycline regulates M1/M2 microglia polarization via the STAT1/STAT6 pathway.

Minocycline prevented neurons from OGD/R-induced cell death in neuron-microglia co-cultures

To clarify the neuroprotective role of modulating microglia polarization, we directly added primary cortical microglia to co-cultures of primary neurons (Fig. 7a). The post-OGD/R neurons were incubated with the different groups of primary microglia. The neurons from minocycline-pretreated M1 microglia with LPS plus IFN-γ attenuated OGD/R-induced neuron damage compared to the M1 microglia with LPS plus IFN-γ, revealed by increasing cell viability (P < 0.0001; Fig. 7b) and reduced LDH release (P = 0.0019; Fig. 7c). The results show that minocycline ameliorates neuronal cell death via modulating microglial polarization, contributing to brain functional recovery after ischemic stroke.

Discussion

Numerous studies have shown the neuroprotective effects of minocycline in ischemic stroke. In particular, both experimental [28, 29] and clinical evidence [30-32] indicate that repeated minocycline treatment can improve functional outcomes after AIS. Previous studies in our laboratory's experimental stroke have shown that minocycline suppresses microglial activation via regulating NLRP3 inflammasome activation [17] and promotes BDNF expression via inhibiting miR-155-mediated repression [24]. Here, using the MCAO/R model, we confirmed that a two-week treatment with minocycline could increase the survival rate and promoted functional outcomes through alleviating neuronal injury and reactive gliosis. We further observed an additive effect of minocycline on microglia polarization to the M1 and M2

phenotypes *in vitro* and *in vivo*. Thus, we demonstrated for the first time that minocycline promoted microglial M2 polarization and inhibited M1 polarization, leading to neuronal survival and neurological functional recovery.

Microglia activation and monocyte infiltration normally peak 48 - 72 h after stroke onset and last for several weeks [33]. In the present study, since the mice's deaths occurred in the first week, we observed the involvement of microglia in ischemic injury on 3 d and 7 d after MCAO/R. We found the proliferation and activation of Iba-1$^+$ cells (macrophage/microglia) in the ipsilateral cortex and striatum after MCAO/R. Interestingly, most activated microglia were present around the lesion site on day 3 and then infiltrated the ischemic core on day 7, indicating that microglia may clear the cell debris by phagocytosis crucially in the resolution of inflammation. As previously reported [26, 33], both CD16/32 and CD206 were detected in the mouse brain on day 7 after MCAO/R, while both M1 markers (IL-1β, IL-6, iNOS, and TNF-α) and M2 markers (Arg1, IL-10, TGF-β, and Ym1) were observed. These results demonstrated an M1/M2 polarization microglia/macrophages in the ipsilateral hemisphere of MCAO/R mice. Furthermore, we found that the number of M1 microglia in the penumbral was much larger than the number of M2 microglia on day 7 after MCAO/R. A previous study reported an M2-to-M1 transition in microglia/macrophages in the ischemic core [34]. During the first two weeks after the onset of ischemic stroke, M1 microglia has increased in the ischemic core over time, whereas M2 microglia arrives at the peak at day 5 and then intensively decreased throughout the second week. The long-term activation of M1 microglia can lead to secondary neuronal damage in the next few months. Our results were consistent with these findings and further indicated that minocycline reverses this M2-to-M1 transition. The experiment *in vitro* further revealed that minocycline reduced microglial M1 polarization and promoted M2 polarization. We also found that microglia treated with minocycline prevented OGD/R-induced neuronal cell death in the neuron-microglia co-cultures. Thus, one novel finding in the present study is that minocycline reversed ischemic-induced M2-to-M1 transition and alleviated neuronal injury in experimental stroke, suggesting that minocycline shifts microglia from M1 to M2 phenotype to improve functional recovery after cerebral ischemia.

Numerous studies reported a critical role of minocycline in the suppression of microglial activation. Minocycline could selectively attenuate M1 polarization of microglia via inhibiting the upregulation of NF-κB in the LPS-stimulated microglia and SOD1(G93A) mice [35]. Chronic administration of minocycline modulates the gene expression of M1-M2 microglial to attenuate neuropathic pain behavior in a rat model of depression [36]. Recently, the results of a single systemic injection of LPS showed that minocycline inhibited neuroinflammatory responses and promoted M2 polarization of microglia through activation SIRT1 [37]. However, the underlying mechanism of minocycline in regulating microglia polarization after stroke is unknown. The Janus kinase (JAK)/STAT signaling pathway is a crucial mediator of neuroinflammation and plays an important role in the progression and pathogenesis of ischemic stroke [38]. Both STAT1 and STAT6 contribute to an ischemia-induced switch for microglial activation [38]. Microglia can be polarized to M1 phenotype via STAT1 activation while to M2 phenotype via STAT6 activation. In the present study, LPS plus IFN-γ induced the M1 microglia polarization, resulting

in the STAT1 activation and increased IFN-γ-dependent gene for M1 polarization such as IL-1β, IL-6, iNOS, and TNF-α. Previous studies demonstrate that IFN-γ also suppresses the recruitment of STAT6 to the IL-4R and inhibits its phosphorylation in Th1 cells [39]. We only observed the IFN-γ-induced decreased Arg1 gene, not other M2-related genes or the phosphorylation of STAT6 *in vivo* and *in vitro*. In the present study, minocycline suppressed the phosphorylation of STAT1 and activated the phosphorylation of STAT6, indicating that minocycline regulates M1/M2 microglia polarization via the STAT1/STAT6 pathway.

Conclusion

We demonstrated for the first time that minocycline improved functional recovery after cerebral ischemia via shifting microglia from M1 to M2 phenotype. We found that minocycline reduced the production of genes for M1 polarization and enhanced the expression of genes for M2 polarization through regulating the STAT1 and STAT6 signaling. It would be an important topic that requires further investigation on how minocycline regulates the balance of STAT1 and STAT6 activation in microglia after cerebral ischemia.

Abbreviations

AIS: Acute ischemic stroke

Arg1: Arginase 1

DAB: 3,3'-diaminobenzidine

GAPDH: Glyceraldehyde-3-phosphate dehydrogenase

GFAP: Glial fibrillary acidic protein

IFN-γ: Interferon-γ

IL-1β: Interleukin-1 beta

IL-4: Interleukin-4

IL-6: Interleukin-6

IL-10: Interleukin-10

iNOS: inducible nitric oxide synthase

IV-tPA: Intravenous thrombolysis with recombinant tissue-type plasminogen activator

JAK: Janus kinase

LPS: Lipopolysaccharide

MCAO/R: Transient middle cerebral artery occlusion - reperfusion

NF-κB: Nucleus factor-kappa-light-chain-enhancer of activated B cells

NLRP3: NLR family pyrin domain containing 3

NSS: Neurological severity scores

OGD/R: Oxygen-glucose deprivation/reperfusion

qRT-PCR: Quantitative real-time polymerase chain reaction

STAT1: Signal transducer and activator of transcription 1

STAT6: Signal transducer and activator of transcription 6

TTC: Triphenyl tetrazolium chloride

TNF-α: Tumor necrosis factor-alpha

TGF-β: Transforming growth factor-beta

Declarations

Ethics approval and consent to participate

All experimental procedures were approved by the Institutional Animal Care and Use Committee of Nanjing Medical University.

Consent for publication

Not applicable.

Availability of data and materials

Not applicable.

Competing interests

The authors declare that they have no competing interests.

Funding

This study was supported by grants from the Key Program of Nantong University Clinical Medicine Special Project (No. 2019JZ020 to Y.H.), the Wuxi Project of Health Commission (No. M202017 to Y.L.), and the Wuxi Double Hundred Training Projects for Young and Middle-aged Medical Top Talents (to Y.L.).

Authors' contributions

YH and YF designed the research; Y-nL, MZ, Y(un)L, and Y(an)L performed the research; Y-nL and Y(an)L analyzed the data; YH and YF wrote the manuscript, and all authors revised the manuscript.

Acknowledgements

Not applicable.

References

1. Donkor ES. Stroke in the 21(st) Century: A Snapshot of the Burden, Epidemiology, and Quality of Life. Stroke Res Treat. 2018;2018:3238165.
2. Phipps MS, Cronin CA. Management of acute ischemic stroke. BMJ. 2020;368:l6983.
3. Catanese L, Tarsia J, Fisher M. Acute Ischemic Stroke Therapy Overview. Circ Res. 2017;120(3):541-58.
4. Ciccone A, Valvassori L, Nichelatti M, Sgoifo A, Ponzio M, Sterzi R, et al. Endovascular treatment for acute ischemic stroke. N Engl J Med. 2013;368(10):904-13.
5. Khatri P, Yeatts SD, Mazighi M, Broderick JP, Liebeskind DS, Demchuk AM, et al. Time to angiographic reperfusion and clinical outcome after acute ischaemic stroke: an analysis of data from the Interventional Management of Stroke (IMS III) phase 3 trial. Lancet Neurol. 2014;13(6):567-74.
6. Cirillo C, Brihmat N, Castel-Lacanal E, Le Friec A, Barbieux-Guillot M, Raposo N, et al. Post-stroke remodeling processes in animal models and humans. J Cereb Blood Flow Metab. 2020;40(1):3-22.
7. Jayaraj RL, Azimullah S, Beiram R, Jalal FY, Rosenberg GA. Neuroinflammation: friend and foe for ischemic stroke. J Neuroinflammation. 2019;16(1):142.
8. Ma Y, Wang J, Wang Y, Yang GY. The biphasic function of microglia in ischemic stroke. Prog Neurobiol. 2017;157:247-72.
9. Zhang W, Tian T, Gong SX, Huang WQ, Zhou QY, Wang AP, et al. Microglia-associated neuroinflammation is a potential therapeutic target for ischemic stroke. Neural Regen Res. 2021;16(1):6-11.
10. Zhao SC, Ma LS, Chu ZH, Xu H, Wu WQ, Liu F. Regulation of microglial activation in stroke. Acta Pharmacol Sin. 2017;38(4):445-58.
11. Wang J, Xing H, Wan L, Jiang X, Wang C, Wu Y. Treatment targets for M2 microglia polarization in ischemic stroke. Biomed Pharmacother. 2018;105:518-25.
12. Kanazawa M, Ninomiya I, Hatakeyama M, Takahashi T, Shimohata T. Microglia and Monocytes/Macrophages Polarization Reveal Novel Therapeutic Mechanism against Stroke. Int J Mol Sci. 2017;18(10).
13. Romero-Miguel D, Lamanna-Rama N, Casquero-Veiga M, Gomez-Rangel V, Desco M, Soto-Montenegro ML. Minocycline in neurodegenerative and psychiatric diseases: an update. Eur J

Neurol. 2020.
14. Zhou YQ, Liu DQ, Chen SP, Sun J, Wang XM, Tian YK, et al. Minocycline as a promising therapeutic strategy for chronic pain. Pharmacol Res. 2018;134:305-10.
15. Garrido-Mesa N, Zarzuelo A, Galvez J. Minocycline: far beyond an antibiotic. Br J Pharmacol. 2013;169(2):337-52.
16. Malhotra K, Chang JJ, Khunger A, Blacker D, Switzer JA, Goyal N, et al. Minocycline for acute stroke treatment: a systematic review and meta-analysis of randomized clinical trials. J Neurol. 2018;265(8):1871-9.
17. Lu Y, Xiao G, Luo W. Minocycline Suppresses NLRP3 Inflammasome Activation in Experimental Ischemic Stroke. Neuroimmunomodulation. 2016;23(4):230-8.
18. Padma Srivastava MV, Bhasin A, Bhatia R, Garg A, Gaikwad S, Prasad K, et al. Efficacy of minocycline in acute ischemic stroke: a single-blinded, placebo-controlled trial. Neurol India. 2012;60(1):23-8.
19. Kohler E, Prentice DA, Bates TR, Hankey GJ, Claxton A, van Heerden J, et al. Intravenous minocycline in acute stroke: a randomized, controlled pilot study and meta-analysis. Stroke. 2013;44(9):2493-9.
20. Yarnell AM, Barry ES, Mountney A, Shear D, Tortella F, Grunberg NE. The Revised Neurobehavioral Severity Scale (NSS-R) for Rodents. Curr Protoc Neurosci. 2016;75:9 52 1-9 16.
21. Shu ZM, Shu XD, Li HQ, Sun Y, Shan H, Sun XY, et al. Ginkgolide B Protects Against Ischemic Stroke Via Modulating Microglia Polarization in Mice. CNS Neurosci Ther. 2016;22(9):729-39.
22. Manwani B, Liu F, Xu Y, Persky R, Li J, McCullough LD. Functional recovery in aging mice after experimental stroke. Brain Behav Immun. 2011;25(8):1689-700.
23. Zhang J, Yang B, Sun H, Zhou Y, Liu M, Ding J, et al. Aquaporin-4 deficiency diminishes the differential degeneration of midbrain dopaminergic neurons in experimental Parkinson's disease. Neurosci Lett. 2016;614:7-15.
24. Lu Y, Huang Z, Hua Y, Xiao G. Minocycline Promotes BDNF Expression of N2a Cells via Inhibition of miR-155-Mediated Repression After Oxygen-Glucose Deprivation and Reoxygenation. Cell Mol Neurobiol. 2018;38(6):1305-13.
25. Sun H, Liang R, Yang B, Zhou Y, Liu M, Fang F, et al. Aquaporin-4 mediates communication between astrocyte and microglia: Implications of neuroinflammation in experimental Parkinson's disease. Neuroscience. 2016;317:65-75.
26. Hu X, Li P, Guo Y, Wang H, Leak RK, Chen S, et al. Microglia/macrophage polarization dynamics reveal novel mechanism of injury expansion after focal cerebral ischemia. Stroke. 2012;43(11):3063-70.
27. Labonte AC, Tosello-Trampont AC, Hahn YS. The role of macrophage polarization in infectious and inflammatory diseases. Mol Cells. 2014;37(4):275-85.
28. Machado LS, Sazonova IY, Kozak A, Wiley DC, El-Remessy AB, Ergul A, et al. Minocycline and tissue-type plasminogen activator for stroke: assessment of interaction potential. Stroke. 2009;40(9):3028-

33.
29. Murata Y, Rosell A, Scannevin RH, Rhodes KJ, Wang X, Lo EH. Extension of the thrombolytic time window with minocycline in experimental stroke. Stroke. 2008;39(12):3372-7.
30. Fagan SC, Waller JL, Nichols FT, Edwards DJ, Pettigrew LC, Clark WM, et al. Minocycline to improve neurologic outcome in stroke (MINOS): a dose-finding study. Stroke. 2010;41(10):2283-7.
31. Lampl Y, Boaz M, Gilad R, Lorberboym M, Dabby R, Rapoport A, et al. Minocycline treatment in acute stroke: an open-label, evaluator-blinded study. Neurology. 2007;69(14):1404-10.
32. Amiri-Nikpour MR, Nazarbaghi S, Hamdi-Holasou M, Rezaei Y. An open-label evaluator-blinded clinical study of minocycline neuroprotection in ischemic stroke: gender-dependent effect. Acta Neurol Scand. 2015;131(1):45-50.
33. Perego C, Fumagalli S, De Simoni MG. Temporal pattern of expression and co-localization of microglia/macrophage phenotype markers following brain ischemic injury in mice. J Neuroinflammation. 2011;8:174.
34. Taylor RA, Sansing LH. Microglial responses after ischemic stroke and intracerebral hemorrhage. Clin Dev Immunol. 2013;2013:746068.
35. Kobayashi K, Imagama S, Ohgomori T, Hirano K, Uchimura K, Sakamoto K, et al. Minocycline selectively inhibits M1 polarization of microglia. Cell Death Dis. 2013;4(3):e525.
36. Burke NN, Kerr DM, Moriarty O, Finn DP, Roche M. Minocycline modulates neuropathic pain behaviour and cortical M1-M2 microglial gene expression in a rat model of depression. Brain Behav Immun. 2014;42:147-56.
37. Wu LH, Huang BR, Lai SW, Lin C, Lin HY, Yang LY, et al. SIRT1 activation by minocycline on regulation of microglial polarization homeostasis. Aging (Albany NY). 2020;12(18):17990-8007.
38. Deszo EL, Brake DK, Kelley KW, Freund GG. IL-4-dependent CD86 expression requires JAK/STAT6 activation and is negatively regulated by PKCdelta. Cell Signal. 2004;16(2):271-80.
39. Huang Z, Xin J, Coleman J, Huang H. IFN-gamma suppresses STAT6 phosphorylation by inhibiting its recruitment to the IL-4 receptor. J Immunol. 2005;174(3):1332-7.

Tables

Table 1. the neurological severity scores (NSS) system for the mice MCAO/R model.

Hemiplegia	
Adapted from contralateral forelimb flexion (left forelimb)	yes 1 no 0
Adapted from contralateral hindlimb flexion (left hindlimb)	yes 1 no 0
Head moved −10° to vertical axis within 30 s	yes 1 no 0
Mobility	
normal walk	yes 0
Lobster walking	yes 1
Circling toward the paretic side (right side)	yes 2
Failure in walking	yes 3
Stability on beam-balancing	
Able to walk, normal gait	yes 0
Able to walk, impaired gait (abnormal walking)	yes 1
Unable to walk, steady balance on beam (be hanging on forelimb lift on the board)	yes 2
Unable to walk, steady balance on beam (all limbs out beam)	yes 3
Unable to stay on the board ($t \geq 40$ s)	yes 4
Unable to stay on the board ($20\ s \leq t < 40$ s)	yes 5
Unable to stay on the board ($t < 20$ s)	yes 6

Figures

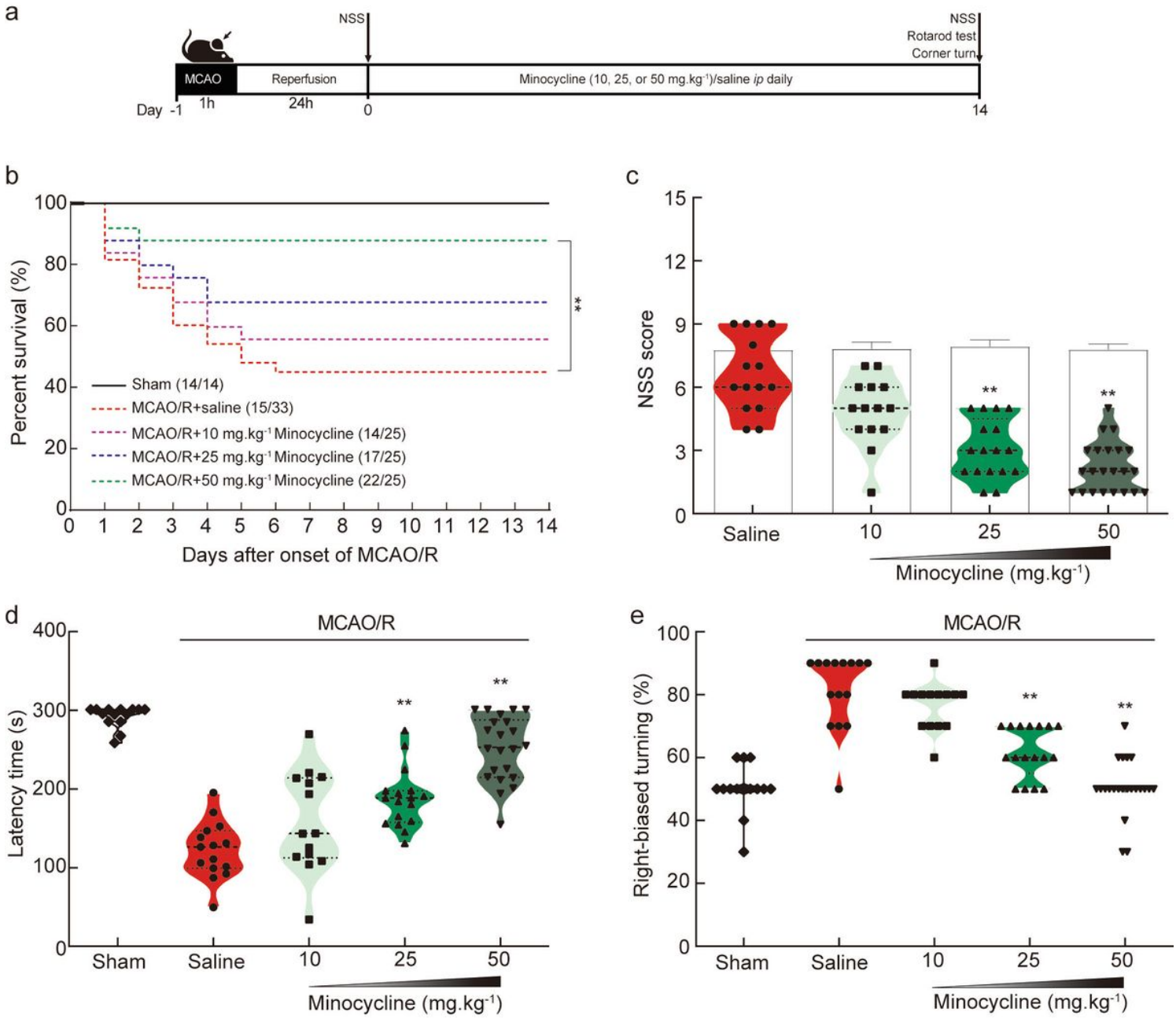

Figure 1

Minocycline enhanced functional recovery on day 14 after MCAO/R model. a Diagram of the experimental procedure. According to the neurological severity scores (NSS) system, mice were randomly divided into 4 groups and received daily intraperitoneal injections with saline, minocycline 10 mg/kg, 20 mg/kg, or 50 mg/kg after 24 h of reperfusion. Neurobehavioral evaluation, rotarod test, and corner turning test were carried out at d 14 after reperfusion. b The survival percentages of the mice suffered from MCAO/R with different minocycline concentrations. Mean ± S.E.M. **P < 0.01 vs. MCAO/R + saline group. Statistical analysis was carried out with a log-rank test. c The NSS score of mice treated with different minocycline concentrations on day 1 (open column) and day 14 after MCAO/R. Mean ± S.E.M. **P < 0.01 vs. MCAO/R + saline group (Saline). Statistical analysis was carried out with a non-parametric Kruskal-Wallis H-test. d The latency time in the rotarod test on day 14 after MCAO/R. Mean ± S.E.M. **P < 0.01 vs.

MCAO/R + saline group (Saline). Statistical analysis was carried out with a one-way analysis of variance followed by Tukey's test. e The percentage of right-biased turning in the corner turning test on day 14 after MCAO/R. Mean ± S.E.M. **P < 0.01 vs. MCAO/R + saline group (Saline). Statistical analysis was carried out with a one-way analysis of variance followed by Tukey's test.

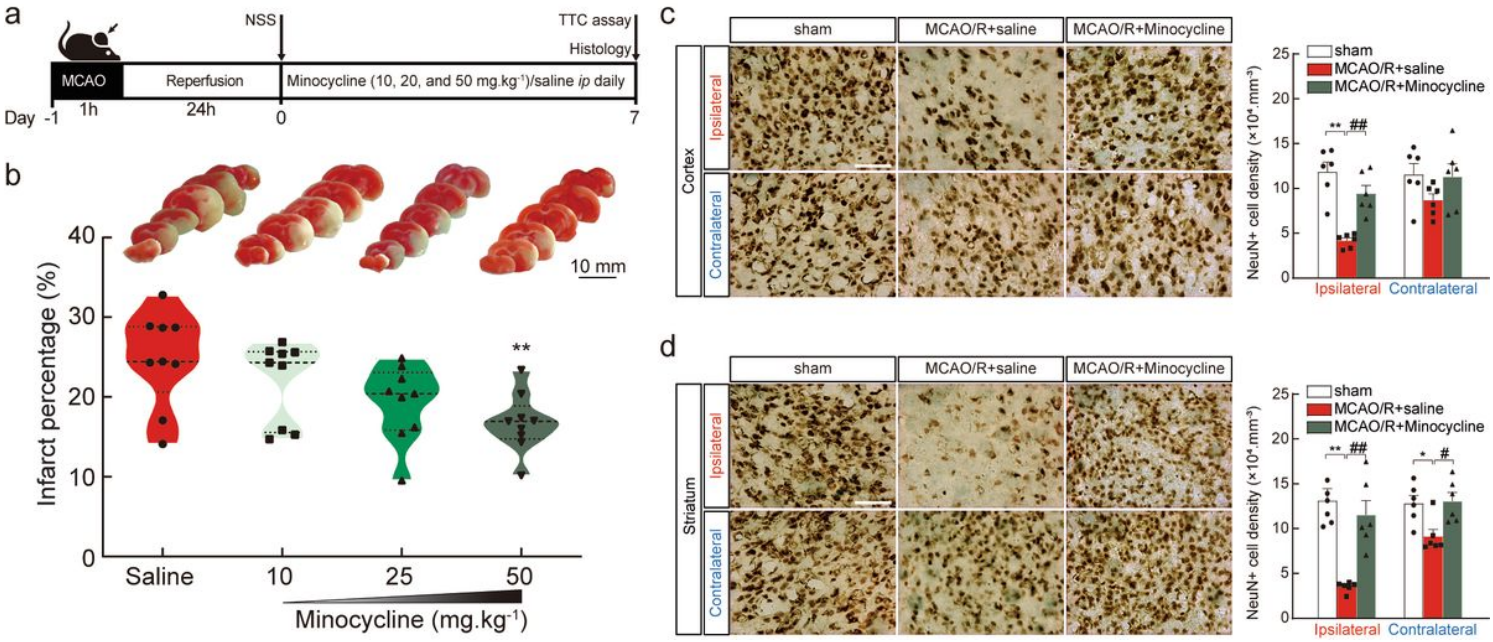

Figure 2

Minocycline alleviated neuronal injury on day 7 after MCAO/R model. a Diagram of the experimental procedure. TTC assay and immunohistochemistry were carried out on day 7 after reperfusion. b Representative images (Upper) of TTC-stained coronal slices on day 7 after reperfusion from four groups. The infarct percentage of the cerebral hemisphere (Lower) in four groups. Mean ± S.E.M. n = 9. **P < 0.01 vs. MCAO/R + saline group (Saline). Statistical analysis was carried out with a one-way analysis of variance followed by Tukey's test. c Representative images (Left) of NeuN+ cells in the cortex on day 7 after reperfusion from sham, MCAO/R + saline, and MCAO/R + 50 mg/kg minocycline (MCAO/R + Minocycline) groups. The NeuN+ cell density in the cortex (Right) in three groups. Scar bar: 200 μm. Mean ± S.E.M. n = 6. **P < 0.01 vs. sham group. ##P < 0.01 vs. MCAO/R + saline group. Statistical analysis was carried out with a one-way analysis of variance followed by Tukey's test. d Representative images (Left) of NeuN+ cells in the striatum on day 7 after reperfusion from sham, MCAO/R + saline, and MCAO/R + 50 mg/kg minocycline (MCAO/R + Minocycline) groups. The NeuN+ cell density in the striatum (Right) in three groups. Scar bar: 200 μm. Mean ± S.E.M. n = 6. *P < 0.05, **P < 0.01 vs. sham group; #P < 0.05, ##P < 0.01 vs. MCAO/R + saline group. Statistical analysis was carried out with a one-way analysis of variance followed by Tukey's test.

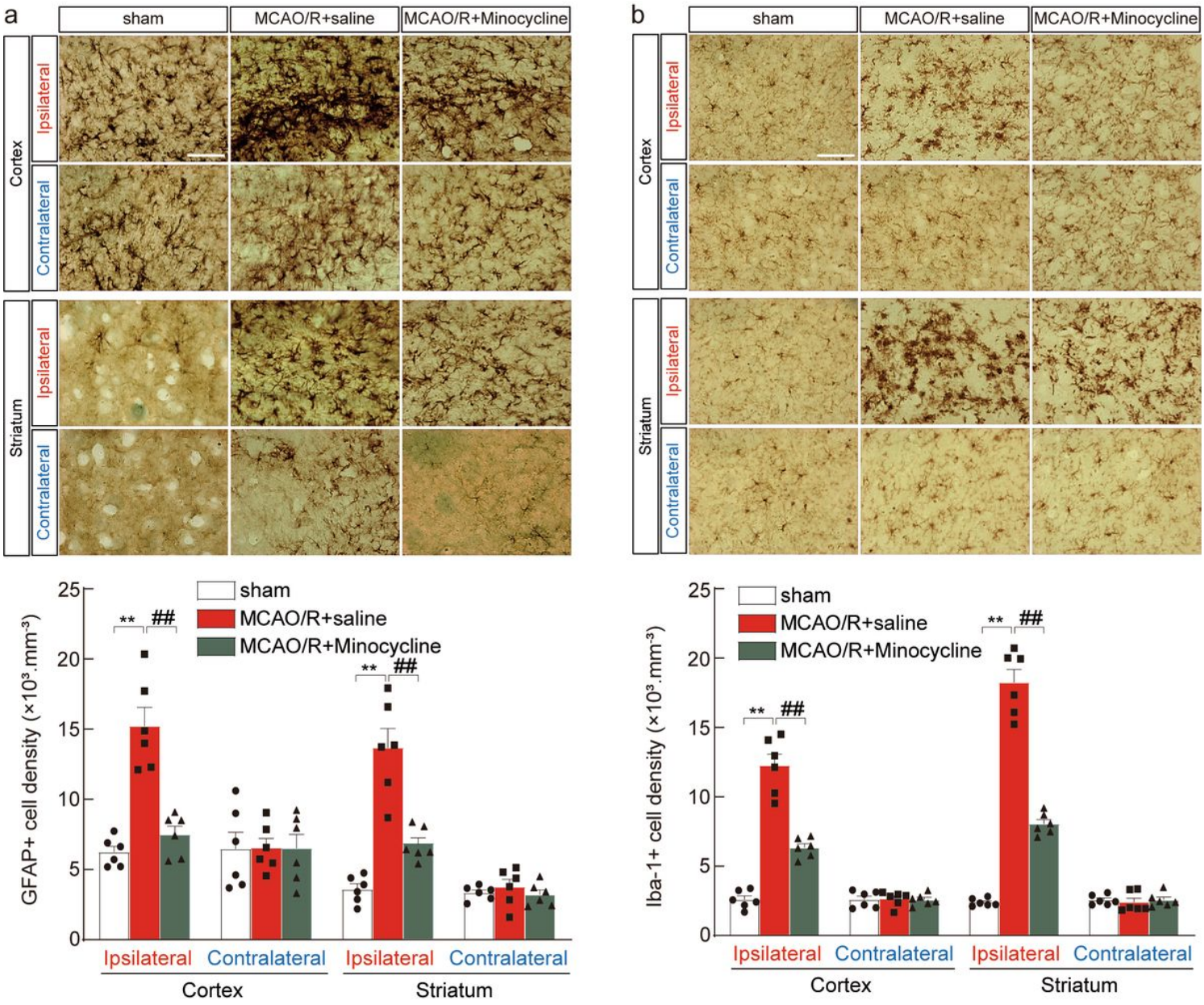

Figure 3

Minocycline reduced reactive gliosis on day 7 after MCAO/R model. a Representative images (Upper) of GFAP+ cells in the cortex and striatum on day 7 after reperfusion from sham, MCAO/R + saline, and MCAO/R + 50 mg/kg minocycline (MCAO/R + Minocycline) groups. The GFAP+ cell density in the cortex and striatum (Lower) in three groups. Scar bar: 200 μm. Mean ± S.E.M. n = 6. **P < 0.01 vs. sham group. ##P < 0.01 vs. MCAO/R + saline group. Statistical analysis was carried out with a one-way analysis of variance followed by Tukey's test. b Representative images (Upper) of Iba-1+ cells in the cortex and striatum on day 7 after reperfusion from sham, MCAO/R + saline, and MCAO/R + 50 mg/kg minocycline (MCAO/R + Minocycline) groups. The Iba-1+ cell density in the cortex and striatum (Lower) in three groups. Scar bar: 200 μm. Mean ± S.E.M. n = 6. **P < 0.01 vs. sham group; ##P < 0.01 vs. MCAO/R + saline group. Statistical analysis was carried out with a one-way analysis of variance followed by Tukey's test.

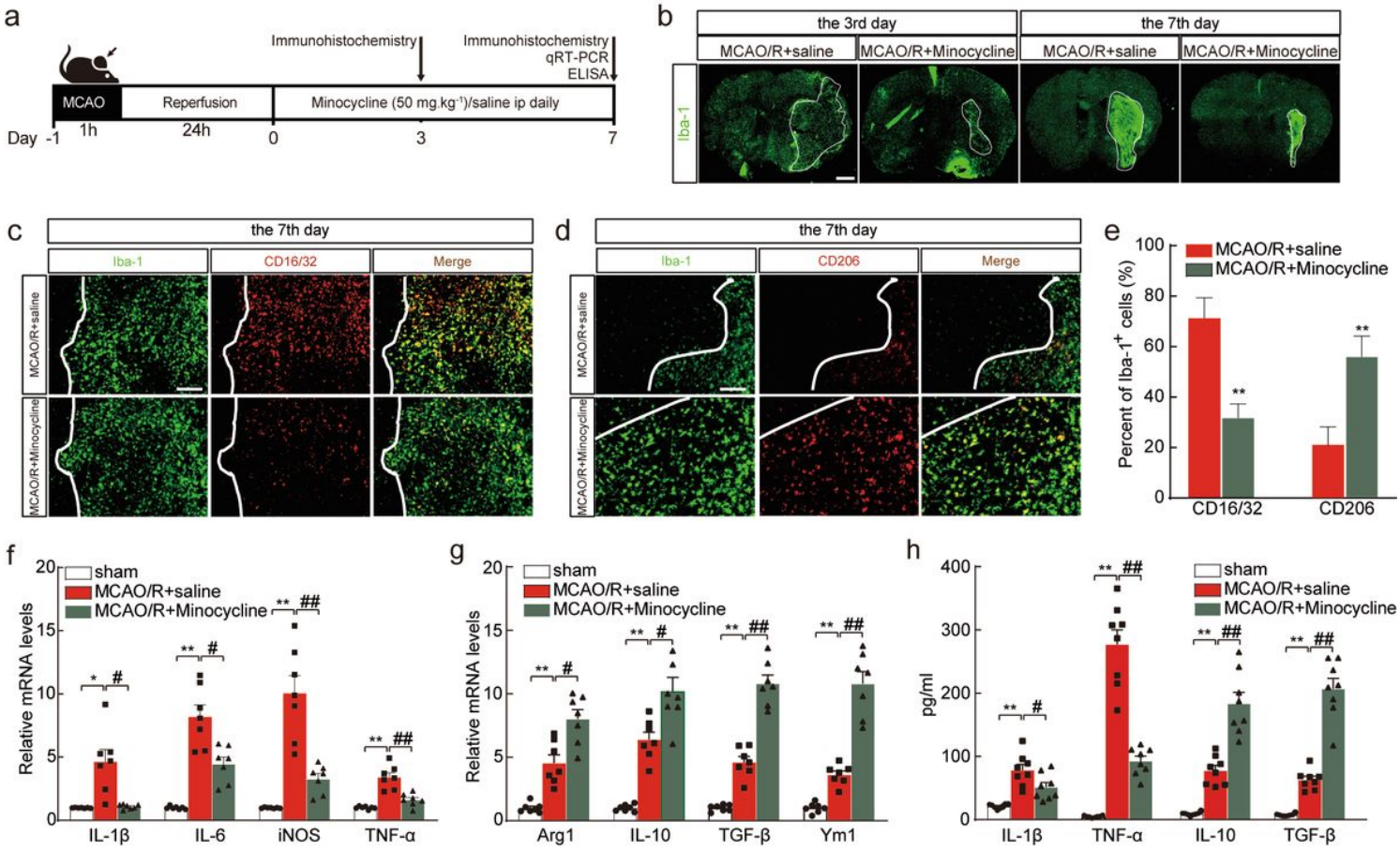

Figure 4

Minocycline promoted M2 macrophage/microglia polarization on day 7 after MCAO/R model. a Diagram of the experimental procedure. Immunofluorescence was carried out on day 3 and d 7 after reperfusion; qRT-PCR and ELISA were carried out on day 7 after reperfusion. b Representative images of Iba-1-stained coronal slices on day 3 and d 7 after reperfusion from MCAO/R + saline and MCAO/R + 50 mg/kg minocycline (MCAO/R + Minocycline) groups. Scar bar: 1 mm. c Representative double-staining immunofluorescence of CD16/32 and Iba-1 in the penumbra on day 7 after reperfusion from MCAO/R + saline and MCAO/R + 50 mg/kg minocycline (MCAO/R + Minocycline) groups. Scar bar: 200 μm. d Representative double-staining immunofluorescence of CD206 and Iba-1 in the penumbra on day 7 after reperfusion from MCAO/R + saline and MCAO/R + 50 mg/kg minocycline (MCAO/R + Minocycline) groups. Scar bar: 200 μm. e The co-localization rate of CD16/32 or CD206 with Iba-1. Mean ± S.E.M. n = 6. **P < 0.01 vs. MCAO/R + saline group. Statistical analysis was carried out with a two-sample t-test. f Representative M1-related mRNAs change detected by qRT-PCR on day 7 after reperfusion from sham, MCAO/R + saline and MCAO/R + 50 mg/kg minocycline (MCAO/R + Minocycline) groups. Mean ± S.E.M. n = 7. *P < 0.05, **P < 0.01 vs. sham group; #P < 0.05, ##P < 0.01 vs. MCAO/R + saline group. Statistical analysis was carried out with a one-way analysis of variance followed by Tukey's test. g Representative M2-related mRNAs change detected by qRT-PCR on day 7 after reperfusion from sham, MCAO/R + saline and MCAO/R + 50 mg/kg minocycline (MCAO/R + Minocycline) groups. Mean ± S.E.M. n = 7. **P < 0.01 vs. sham group; #P < 0.05, ##P < 0.01 vs. MCAO/R + saline group. Statistical analysis was carried out

with a one-way analysis of variance followed by Tukey's test. h Representative M1 or M2-related cytokines change detected by ELISA on day 7 after reperfusion from sham, MCAO/R + saline and MCAO/R + 50 mg/kg minocycline (MCAO/R + Minocycline) groups. Mean ± S.E.M. n = 8. **P < 0.01 vs. sham group; #P < 0.05, ##P < 0.01 vs. MCAO/R + saline group. Statistical analysis was carried out with a one-way analysis of variance followed by Tukey's test.

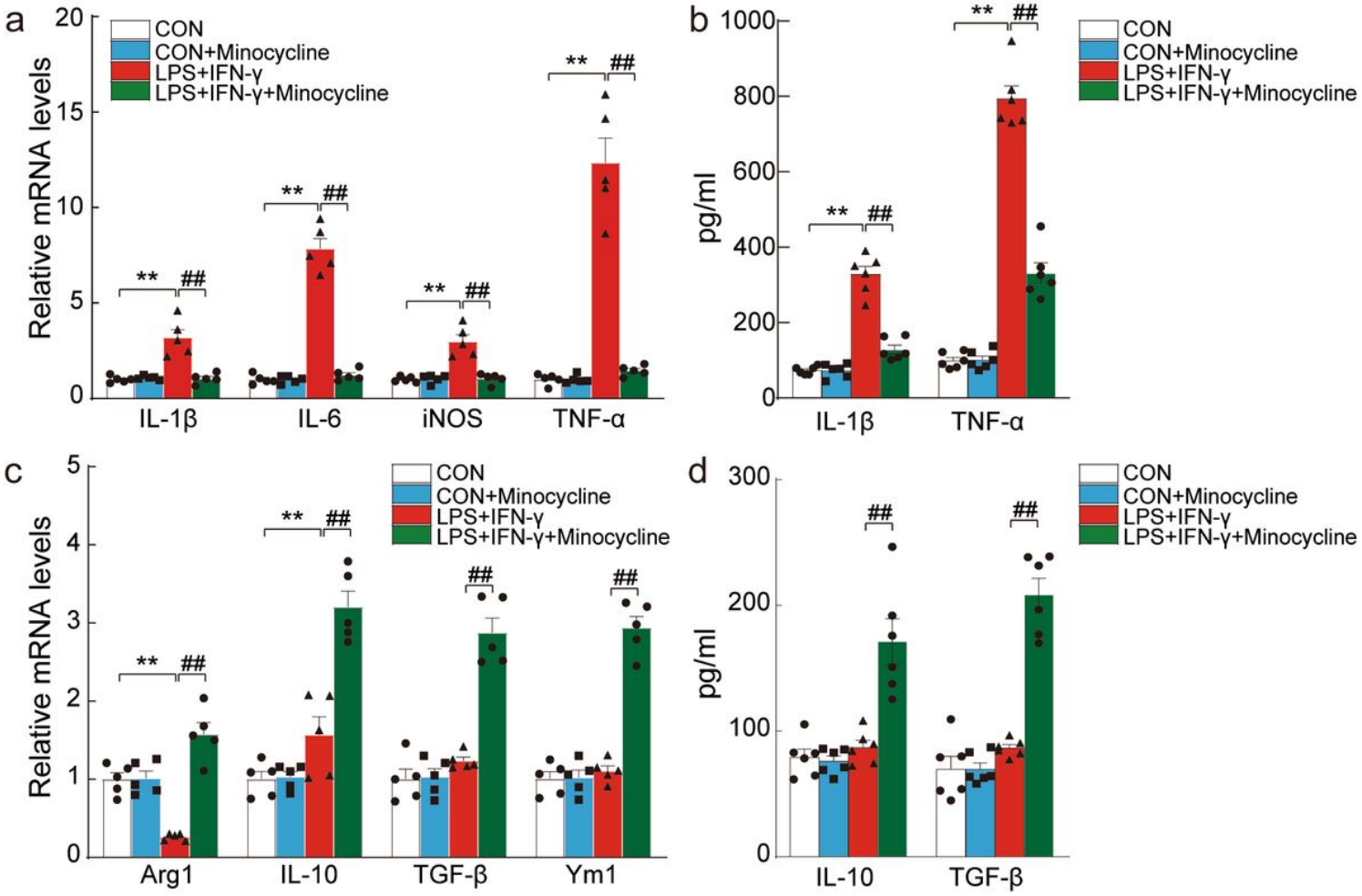

Figure 5

Minocycline facilitated M2 polarization stimulated by LPS and IFN-γ in primary microglia. a Representative M1-related mRNAs change detected by qRT-PCR at 24 h after treatment with LPS and IFN-γ. Mean ± S.E.M from four independent experiments. *P < 0.05, **P < 0.01 vs. control group (CON); #P < 0.05, ##P < 0.01 vs. LPS + IFN-γ group. Statistical analysis was carried out with a one-way analysis of variance followed by Tukey's test. b Representative M1-related cytokines change detected by ELISA at 24 h after treatment with LPS and IFN-γ. Mean ± S.E.M from four independent experiments. *P < 0.05, **P < 0.01 vs. control group (CON); #P < 0.05, ##P < 0.01 vs. LPS + IFN-γ group. c Representative M2-related mRNAs change detected by qRT-PCR at 24 h after treatment with LPS and IFN-γ. Mean ± S.E.M from four independent experiments. *P < 0.05, **P < 0.01 vs. control group (CON); #P < 0.05, ##P < 0.01 vs. LPS + IFN-γ group. Statistical analysis was carried out with a one-way analysis of variance followed by Tukey's test. d Representative M2-related cytokines change detected by ELISA at 24 h after treatment with LPS

and IFN-γ. Mean ± S.E.M from four independent experiments. *P < 0.05, **P < 0.01 vs. control group (CON); #P < 0.05, ##P < 0.01 vs. LPS + IFN-γ group.

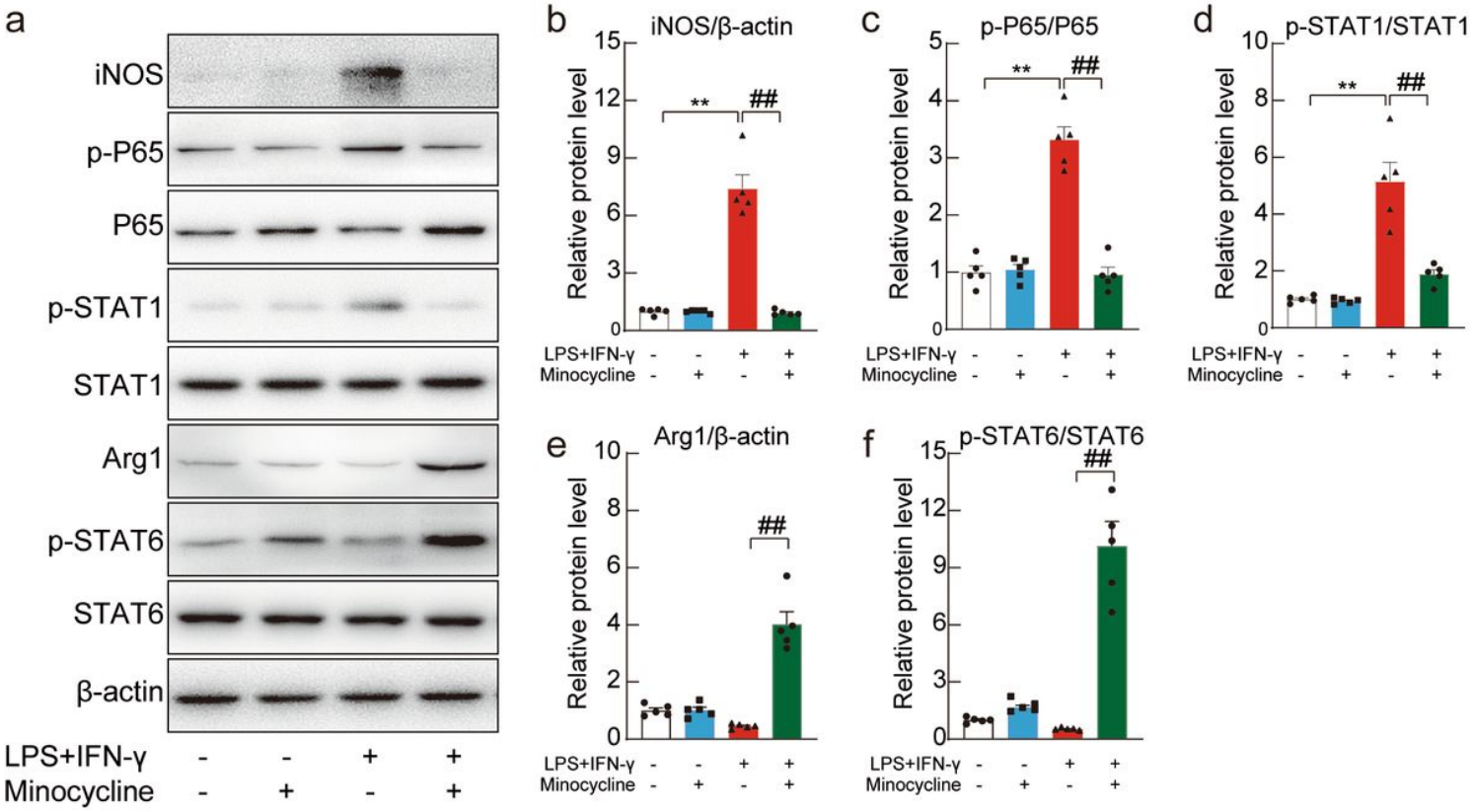

Figure 6

Minocycline regulated M1/M2 polarization via the STAT1/6 signaling pathway in primary microglia. a Representative western blotting images of iNOS, p-P65, P65, p-STAT1, STAT1, Arg1, p-STAT6, STAT6, and β-actin from four groups. β-actin was used as a protein loading control. b The relative protein level of iNOS in four groups. Mean ± S.E.M from four independent experiments. *P < 0.05, **P < 0.01 vs. control group; #P < 0.05, ##P < 0.01 vs. LPS + IFN-γ group. c The relative protein level of p-P65 in four groups. Mean ± S.E.M from four independent experiments. *P < 0.05, **P < 0.01 vs. control group; #P < 0.05, ##P < 0.01 vs. LPS + IFN-γ group. d The relative protein level of p-STAT1 in four groups. Mean ± S.E.M from four independent experiments. *P < 0.05, **P < 0.01 vs. control group; #P < 0.05, ##P < 0.01 vs. LPS + IFN-γ group. e The relative protein level of Arg1 in four groups. Mean ± S.E.M from four independent experiments. #P < 0.05, ##P < 0.01 vs. LPS + IFN-γ group. f The relative protein level of p-STAT6 in four groups. Mean ± S.E.M from four independent experiments. #P < 0.05, ##P < 0.01 vs. LPS + IFN-γ group.

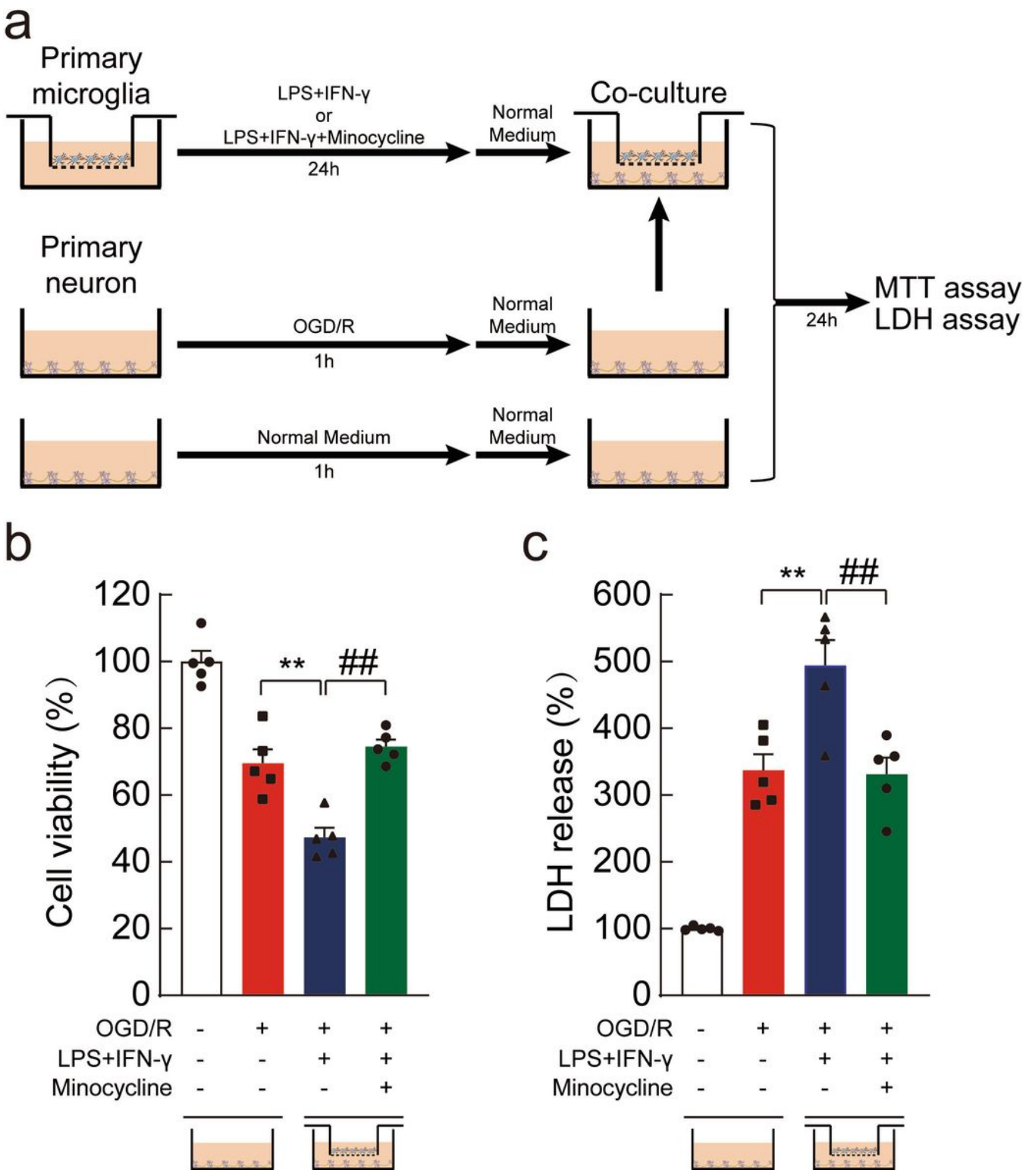

Figure 7

Minocycline prevented neurons from OGD/R-induced cell death in neuron-microglia co-cultures. a Schematic diagram of microglia culture in transwell and OGD/R neuron for 24 h in the absence or presence of 50 μM minocycline. b The cell viability of neurons in four groups. Mean ± S.E.M from five independent experiments. **P < 0.01 vs. OGD/R neuron group; ##P < 0.01 vs. OGD/R neuron and LPS + IFN-γ microglia group. c The LDH release of neurons in four groups. Mean ± S.E.M from five independent

experiments. **P < 0.01 vs. OGD/R neuron group; ##P < 0.01 vs. OGD/R neuron and LPS + IFN-γ microglia group.